# Intrasubject Comparison Between Technetium-99m-ECD and Technetium-99m-HMPAO in Healthy Human Subjects

Jean Léveillé, George Demonceau, and Richard C. Walovitch

*Médecine Nucléaire, Hotel-Dieu de Montréal, Montréal, Canada; Nucleaire Geneeskunde, St. Elisabeth Ziekenhuis, Zottegem, Belgium; and Medical Research, The Du Pont Merck Pharmaceutical Company, N. Billerica, Massachusetts*

The pharmacokinetics and quality of planar and SPECT brain imaging of two $^{99m}$Tc-labeled brain perfusion agents, d,l-hexamethyl propylene amine oxime (HMPAO) and ethyl cysteinate dimer (ECD), were compared in seven healthy, normal subjects. Both radiopharmaceuticals showed rapid brain uptake and had a net brain washout of less than 5% during the first 20 min after drug administration. However, during the same time period, $^{99m}$Tc-ECD images of the head showed significantly less background facial uptake and retention when compared to $^{99m}$Tc-HMPAO images. The brain-to-background contrast ratio of $^{99m}$Tc-ECD (brain/neck) continued to improve over time and by 5 hr postadministration was 17 to 1 versus 2 to 1 for $^{99m}$Tc-HMPAO. SPECT brain images of both agents show gray/white matter ratios that were unchanged over time and an intracerebral distribution consistent with blood flow. A blind read of these SPECT images also shows $^{99m}$Tc-ECD to produce images that were "easier to interpret" with less extracerebral activity as compared to $^{99m}$Tc-HMPAO. Repeat, whole-body planar spot imaging suggests that $^{99m}$Tc-ECD was cleared more rapidly from the body than was $^{99m}$Tc-HMPAO.

**J Nucl Med 1992; 33:480–484**

During the past decade, several neutral, lipophilic radiotracers have been developed for the purpose of imaging regional cerebral perfusion. Of these, the $^{99m}$Tc tracers, most closely meet the desired characteristics for routine clinical use in the tomographic imaging of brain function (*1–3*).

Technetium 99m-HMPAO (Ceretec® Amersham Inc., Amersham UK) was the first and is currently the only $^{99m}$Tc brain perfusion agent commercially available in most countries. It has been validated as a marker of regional cerebral blood flow (*4–6*) and as a valuable adjunct in the diagnosis of various neurological disorders (*1*). Technetium 99m-HMPAO is limited in that its rapid decomposition in vitro necessitates its usage within 30 min of preparation (*7*). Radiochemical stability is not a problem with the newer $^{99m}$Tc brain perfusion agent, $^{99m}$Tc-ethyl cysteinate dimer (ECD) (*8*) (Neurolite®, Du Pont Merck, N. Billerica, MA). Technetium-99m-ECD is presently under clinical evaluation as a marker of regional cerebral perfusion.

Studies in healthy volunteers (*8,9*) and patients (*10–13*) have demonstrated the perfusion distribution pattern and excellent brain imaging characteristics of $^{99m}$Tc-ECD. Previous studies have established the in-vivo kinetics and dosimetry of both agents (*8,9,13,14*). However, information on direct comparison of both agents in the same subject is limited. In a small study of chronic stroke patients, $^{99m}$Tc-ECD images were "easier to read" than $^{99m}$Tc-HMPAO images (*11*). It has been suggested that the superior image quality of $^{99m}$Tc-ECD is mediated in part by a superior brain-to-background and/or brain-to-blood ratio of $^{99m}$Tc-ECD (*11,15,17*). The purpose of this study was to compare the biodistribution, kinetic and SPECT imaging characteristics of $^{99m}$Tc-ECD and $^{99m}$Tc-HMPAO in the same healthy human volunteers.

## METHODS

### Radiopharmaceutical Preparation

Technetium-99m-ECD was prepared as previously described (*8*). The radiochemical purity of the final $^{99m}$Tc-ECD complex was measured by thin-layer chromatography on Whatman MKC18 plates developed with acetone and 0.5 *M* ammonium acetate (60:40). The plates were imaged using a gamma camera. The activity ratio was calculated by comparing the peak for the $^{99m}$Tc-ECD complex to the sum of all other peaks on the plate. A kit formulation of $^{99m}$Tc-HMPAO (Amersham Inc., Amersham UK) was reconstituted and tested for radiochemical purity in accordance with the package insert. Radiochemical purities of 92.2% ± 9% for $^{99m}$Tc-HMPAO and 98.0% ± 1.0% for $^{99m}$Tc-ECD were obtained.

### Imaging Protocol

The protocol was approved by the local ethical committee in each participating institution and written informed consent was obtained from each subject. Each subject (7 males; age range 28–

Received May 29, 1991; revision accepted Nov. 6, 1991.

For reprints contact: Jean Léveillé, MD, FRCP(C), ABNM, Chef Médecine Nucléaire, Hotel-Dieu de Montreal, 3840, rue St-Urbain, Montreal, Quebec H2W 1T8 Canada.

42) completed a medical examination and had no past history of neurological disease. All volunteers received both tracers under identical environmental conditions in random order within a 2–4 day period. On average each subject received 12 mCi or more of $^{99m}$Tc-ECD as compared to $^{99m}$Tc-HMPAO. The difference in injected dose for each radiopharmaceutical was due to differences in radiation dosimetry of each compound. The maximum radiation exposure was set at approximately 3.5 rad to the critical organ (assuming a 2-hr urinary voiding interval), which resulted in a injected dose of approximately 15 mCi for $^{99m}$Tc-HMPAO (Amersham package insert) and 30 mCi for $^{99m}$Tc-ECD (*11*). Intrasubject image acquisition and processing were identical. Immediately after injection of the radiopharmaceutical, dynamic planar brain imaging began using a right lateral view for five volunteers and a frontal view for two volunteers. Data were collected in a 64 × 64 word-mode matrix at a rate of 60 sec per frame for 20 min.

SPECT brain imaging was performed using either a Picker Dyna Digital Camera (DDC)(Picker International, Highland Heights, OH) with a SX-300 detector and a high-resolution collimator or a General Electric GE400-AT camera with a high- or low-energy, high-resolution general-purpose collimator. SPECT studies began at 20, 100, 240, and 360 min after compound administration. Data were collected in a 64 × 64 matrix using 120 angular increments over 360 degrees at 17–20 sec per view. The same tomographic reconstruction was used in each study: Ramp-Hanning filter of 0.5 and spatial filtering after backprojection from the opposite view with an attenuation coefficient of 0.15/cm.

After SPECT brain imaging, anterior whole-body planar images were obtained in multiple areas in a 256 × 256 matrix for 180 sec each. For the first series of whole-body spot images, posterior regions of interest (ROIs) were also determined. Venous blood samples were obtained at 1, 2, 3, 4, 5, 10, 15, 30, 60 min and 24 hr after injection. Urine was collected at 2, 4, 6 and 24 hr after injection.

### Data Analysis

Time-activity curves were generated from dynamic planar images of the head using brain and background facial ROIs. The same ROIs were used for both radiopharmaceuticals. This allowed a direct comparison of the brain to face kinetics for these two agents. Non-brain organ time-activity curves were generated using the same size and shape ROIs for both radiopharmaceuticals. Results were expressed as percent inject dose (%ID) using the gamma camera counting efficiency determined from the phantom studies with a method reported previously (*8*). For the first series of spot images, the organ %ID was determined using the geometric mean of anterior and posterior ROIs. For subsequent image acquisition, only anterior spot images were obtained. In order to calculate %ID, a correction factor was used (%ID anterior spot image ÷ organ specific geometric mean %ID from first spot image). This correction factor was then multiplied by anterior spot image %ID to obtain the final %ID value for all organs.

Blood and urine activities were expressed as %ID. Whole blood volume was obtained from tables based on the height and weight of each subject (*16*). SPECT brain images were analyzed to determine gray/white matter contrast. Representative small box (3 pixel) gray/white matter ROIs were drawn on 2-pixel thick (1.2 cm) slices 6–7 cm above the orbital meatal line (OML). Gray matter regions were defined in the left and right frontal lobes and compared to adjacent left and right periventricular white matter regions.

Visual interpretation of hard copies (x-ray film) of SPECT brain images were performed twice. All transverse slices were displayed so that images were normalized to the hottest pixel in the data set, thus taking into account any differences in image contrast due to the higher injected dose of $^{99m}$Tc-ECD. Initially, all images were examined unblinded using background subtraction which was optimal for that data set. The lower threshold background subtraction was 15%–20% for $^{99m}$Tc-HMPAO and 5% for $^{99m}$Tc-ECD. The upper threshold was the same for both agents (100%).

In the second evaluation, a blind read of the SPECT images was performed by three readers who evaluated paired data sets from the first series of SPECT scans ($^{99m}$Tc-ECD paired with $^{99m}$Tc-HMPAO from the same subject). As a control, images from a chronic stroke patient with a documented left frontal lobe stroke were added to the blind read data set. Background subtraction was uniform with a 5% lower threshold and 100% upper threshold. Images were evaluated to determine the location of perfusion defects, ease of interpretability (extent of gray/white contrast, clarity of brain image) and degree of extracerebral activity. Ease of interpretability and degree of extracerebral activity was determined using a five-point scale, ranging from one (minor difference) to five (major difference) between the two imaging agents.

### Statistical Analysis

Summaries of study variables were expressed as mean ± standard error of the mean (s.e.m.). Analysis of variance with repeated measures was used to compare $^{99m}$Tc-ECD and $^{99m}$Tc-HMPAO. Statistical significance was set at $p = 0.05$.

## RESULTS

Both $^{99m}$Tc-ECD and $^{99m}$Tc-HMPAO showed rapid uptake by the brain. The brain's elimination of both tracers was not significant during the first 20 min of imaging (Fig. 1A), however, $^{99m}$Tc-ECD cleared from background facial tissue more rapidly than $^{99m}$Tc-HMPAO. This resulted in significantly higher brain/neck ratios ($p=0.04$) (Fig. 1B) and clearer brain delineation, particularly in lower brain structures such as the cerebellum (Figs. 2 and 3). Technetium-99m-ECD brain-to-background (neck) activity ratios continued to increase over time as compared with $^{99m}$Tc-HMPAO.

During the first hour after radiopharmaceutical administration, the blood activity (%ID) was higher for $^{99m}$Tc-HMPAO than for $^{99m}$Tc-ECD (Fig. 1C). The higher blood activity was statistically significant at 1, 2, 3, 4, and 60 min postadministration. The kinetics of both radiopharmaceuticals in the brain, legs, liver/gallbladder, lungs and neck are summarized in Figure 4. In general, $^{99m}$Tc-ECD, unlike $^{99m}$Tc-HMPAO, washed out from all regions over time. By 75 min postadministration, the %ID in the lungs and legs was lower for $^{99m}$Tc-ECD than $^{99m}$Tc-HMPAO in all organs, including the brain. Two hours after injection, 62% of the injected $^{99m}$Tc-ECD dose was excreted in the urine compared with 6% of the $^{99m}$Tc-HMPAO dose. The cumulative excreted activity at 24 hr in three subjects was

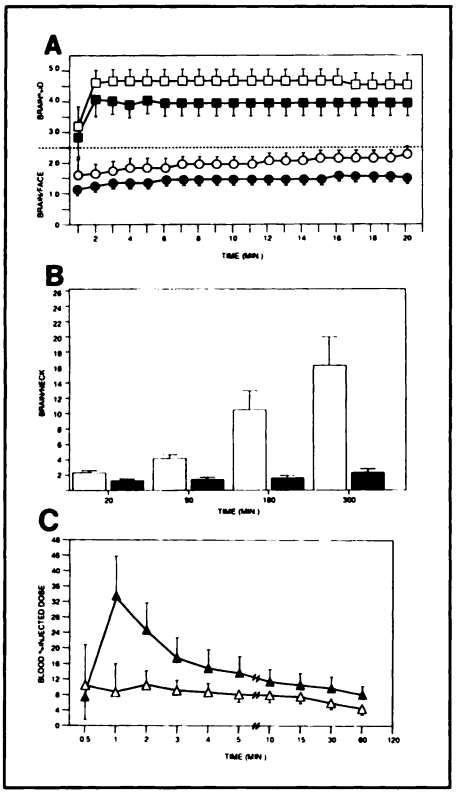


**FIGURE 1.** Within subject comparisons of $^{99m}$Tc-ECD and $^{99m}$Tc-HMPAO in five to six neurologically normal adult males. Open symbols represent $^{99m}$Tc-ECD values as mean ± s.e.m. and closed symbols are $^{99m}$Tc-HMPAO values as mean ± s.e.m. (A). Dynamic planar brain %ID (squares) and brain/face (circles) time-activity curves during the first 20 min postintravenous administration. Note the rapid uptake and stable brain distribution of both compounds (B), brain/neck ratios showing the significantly greater increase after $^{99m}$Tc-ECD as compared to $^{99m}$Tc-HMPAO (C), venous blood %ID of $^{99m}$Tc-ECD and $^{99m}$Tc-HMPAO. Note the faster washout of $^{99m}$Tc-ECD.

79.36% ± 8.68% for $^{99m}$Tc-ECD and 13.6% ± 7.20% for $^{99m}$Tc-HMPAO.

The distribution of activity for both tracers in vascular territories of the brain was similar and remained stable for at least 6 hr after injection. No differences between image quality of $^{99m}$Tc-ECD and $^{99m}$Tc-HMPAO were noted in

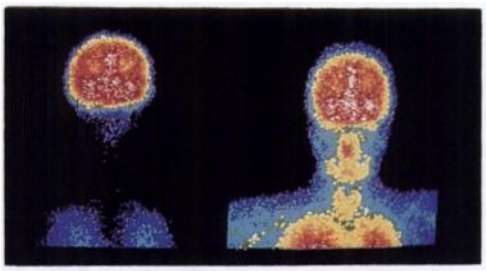

**FIGURE 2.** Anterior planar images of an adult male after administration of $^{99m}$Tc-ECD (left) or $^{99m}$Tc-HMPAO (right). Each image has been thresholded to its maximal pixel value. Note the superior brain-to-background facial tissue ratio for $^{99m}$Tc-ECD.

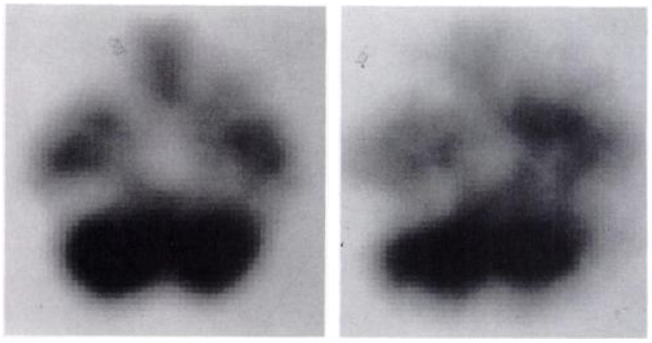

**FIGURE 3.** SPECT brain images (approximately 1 cm above the orbitomeatal line) of the same neurologically normal volunteer after administration of $^{99m}$Tc-ECD (left) and $^{99m}$Tc-HMPAO (right). All images are thresholded to their maximal pixel value and have a lower threshold of 5% and an upper threshold of 100%. Note the higher degree of non-brain background activity in the $^{99m}$Tc-HMPAO images.

the unblinded (optimally processed) image data sets. This is in part attributed to a greater degree of background subtraction from the $^{99m}$Tc-HMPAO images as compared to the $^{99m}$Tc-ECD images (lower threshold 15%–20% versus 5%, respectively). In contrast, during the blind read, when all images were read with the 5% lower threshold, it was concluded by all blind readers that $^{99m}$Tc-ECD images were more interpretable ("easier to read") and had less extracerebral activity than $^{99m}$Tc-HMPAO images (Fig. 3). All three blind readers rated each $^{99m}$Tc-ECD image as having better image quality than the corresponding $^{99m}$Tc-HMPAO image. On the five-point image quality scale, $^{99m}$Tc-ECD scored 3.9 ± 0.3 on image interpretability and 3.9 ± 0.3 on degree of extracerebral activity in question. In one case, one reader said there was no difference in extracerebral activity. All readers correctly identified the

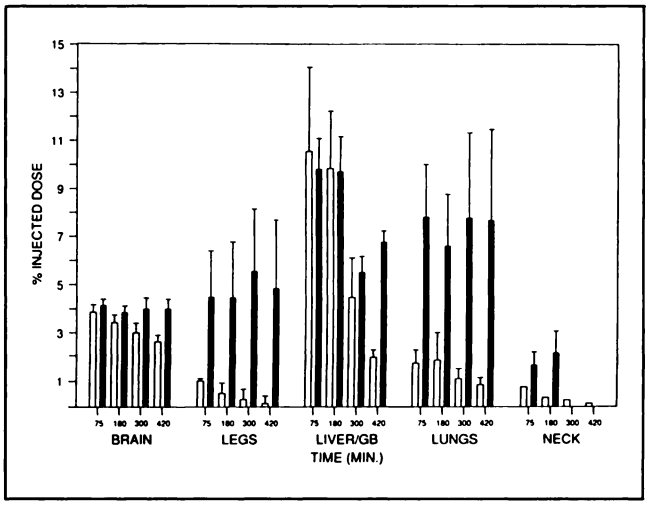


**FIGURE 4.** Within subject comparison of the biodistribution of $^{99m}$Tc-ECD and $^{99m}$Tc-HMPAO in 3–5 subjects. Open symbols represent $^{99m}$Tc-ECD values as mean ± s.e.m. and closed symbols are $^{99m}$Tc-HMPAO values as mean ± s.e.m. In contrast to $^{99m}$Tc-ECD, $^{99m}$Tc-HMPAO shows little washout from all regions.

left frontal lobe defect in both the $^{99m}$Tc-ECD and $^{99m}$Tc-HMPAO images from the chronic stroke patient.

The gray-to-white matter ratios observed within the first hour after drug administration were similar for both $^{99m}$Tc-ECD (1.5 ± 0.07) and $^{99m}$Tc-HMPAO (1.39 ± 0.10) and did not change over time for up to 6 hr after compound administration [gray/white range (1.19–1.88) for $^{99m}$Tc-ECD and for $^{99m}$Tc-HMPAO (1.14–1.92)].

## DISCUSSION

The results of this study show that in neurologically normal subjects, the cerebral kinetics and initial distribution of both $^{99m}$Tc-ECD and $^{99m}$Tc-HMPAO are similar. Postinjection, both agents undergo rapid uptake in brain tissue with a pattern of distribution which is unchanged over time and consistent with perfusion. Technetium-99m-HMPAO is retained in the brain longer than $^{99m}$Tc-ECD, but brain retention of $^{99m}$Tc-ECD is sufficient so that high quality single-head rotating gamma camera SPECT brain imaging studies may be performed (*8,13*).

In contrast to $^{99m}$Tc-HMPAO, the brain-to-soft-tissue activity ratios of $^{99m}$Tc-ECD continue to increase with time (Fig. 1A,B). Technetium-99m-ECD was cleared from the blood more rapidly than was $^{99m}$Tc-HMPAO (Fig. 1C). The biodistribution of $^{99m}$Tc-ECD also suggests that it is eliminated more rapidly than $^{99m}$Tc-HMPAO from most tissues. The rapid and extensive renal excretion of $^{99m}$Tc-ECD as compared to $^{99m}$Tc-HMPAO (79% versus 14% ID) supports the dosimetry of $^{99m}$Tc-ECD, which shows the urinary bladder wall to be the dose-limiting organ [0.11 rad/mCi with a 2-hr voiding interval (*9*)]. In contrast, the major route of excretion of $^{99m}$Tc-HMPAO is hepatobiliary. The absorbed radiation dose of 0.258 rad/mCi for the dose-limiting organ, the lachrymal gland (Amersham package insert for Ceretec®), is more than double that of $^{99m}$Tc-ECD.

In this study, $^{99m}$Tc-ECD SPECT images had less extracerebral activity and were "easier to interpret" than $^{99m}$Tc-HMPAO images. Similar results have been observed in patients (*10,11,17*). Moretti et al. (*11*) suggest that the more rapid blood elimination of $^{99m}$Tc-ECD as compared to $^{99m}$Tc-HMPAO may be responsible for the $^{99m}$Tc-ECD superior brain lesion-to-normal tissue contrast. In a larger study of 10 dementia and 8 stable stroke patients, Castagnoli et al. (*17*) showed by SPECT brain ROI analysis that $^{99m}$Tc-ECD had superior lesion-to-normal tissue contrast than $^{99m}$Tc-HMPAO in the same patient. In addition, a blind read analysis of those same patients showed that the SPECT brain image quality was superior to that with $^{99m}$Tc-ECD.

It is possible that the superior image quality of $^{99m}$Tc-ECD as compared to $^{99m}$Tc-HMPAO observed by Morretti and Castagnoli could be attributed to the kinetic differences between the two brain agents. For example, a patient with a cortical stroke who has an increase in blood volume and decrease in blood flow may more clearly show a perfusion defect if imaged with an agent that has little glandular uptake and low blood activity. Conversely, the inferior lesion contrast of $^{99m}$Tc-HMPAO in acute stroke patients as compared to [$^{123}$I]N-isopropyl-p-iodoamphetamine has been attributed to the high blood activity of $^{99m}$Tc-HMPAO (*18*). In addition, up to 20% of the ID of a Ceretec® kit may be in the form of hydrophilic complexes that may be taken up in infarcted areas where the blood-brain barrier is disrupted. Although it appears that the blood and facial tissue pharmacokinetics for both compounds ($^{99m}$Tc-ECD and $^{99m}$Tc-HMPAO) may play a role in SPECT brain image quality, an understanding of the peak brain extraction fraction, backflux and retention mechanism of $^{99m}$Tc-ECD is needed before any conclusion can be drawn as to why intrasubject differences in SPECT image quality are observable.

There is no evidence that the two-fold higher dose of $^{99m}$Tc-ECD (30 mCi) as compared to $^{99m}$Tc-HMPAO (15 mCi) is responsible for the agents superior image quality. The counting statistics were sufficient enough (five million total counts for $^{99m}$Tc-HMPAO and ten million total counts for $^{99m}$Tc-ECD for a 20–60-min scan) to allow for high quality SPECT images to be obtained in both cases.

A few studies have been conducted comparing the brain extraction of $^{99m}$Tc-ECD to that of $^{99m}$Tc-HMPAO in animal models which show them to be similar (approximately 70% at normal brain blood flow for both compounds) (*3,12*). The retention mechanism of both agents has been studied in healthy brain tissue (*19,20*) but not in pathological tissue. It has been suggested that $^{99m}$Tc-HMPAO is a marker of regional cerebral perfusion in stroke (*21*) and therefore will show the transient hyperemia observed in some cases of subacute stroke. This would result in cerebral infarction being harder to visualize with $^{99m}$Tc-HMPAO. It is not now known if hyperemia is observable after subacute stroke with $^{99m}$Tc-ECD.

In conclusion, our intrasubject comparison in neurologically normal subjects shows that $^{99m}$Tc-ECD and $^{99m}$Tc-HMPAO are rapidly taken up in the brain in a pattern consistent with cerebral perfusion. However, $^{99m}$Tc-ECD is cleared from the body more rapidly than $^{99m}$Tc-HMPAO, which may in part account for the superior SPECT image quality observed in the $^{99m}$Tc-ECD images during the blind read.

## ACKNOWLEDGMENTS

The authors greatly acknowledge Dr. Tsushung A. Hua for statistical advice and technical support with the statistical analysis, Dr. Luc Marchand for performing the blind read and Dr. Stephen Williams and Dr. Norman LaFrance for their advice and helpful comments. We would also like to thank André Gagnon for his technical assistance and Donna Hulub for her invaluable secretarial support in preparing this manuscript.

## REFERENCES

1. Ell PJ, Jarritt PH, Costa DC, Cullum ID, Lui D. Functional imaging of the brain. *Semin Nucl Med* 1987;17:214–229.
2. Shepstone BJ. Cerebral scintigraphy—the phoenix rises again. *Postgrad*

*Med J* 1988;64:4–17.
3. Walovitch RC, Williams SJ, LaFrance ND. Radiolabeled agents for SPECT imaging of brain perfusion. *Nucl Med Biol* 1990;17:77–83.
4. Gemmell HG, Evans NT, Besson JA, et al. Regional cerebral blood flow imaging: a quantitative comparison of technetium-99m-HMPAO SPECT with $C^{15}O_2$ PET. *J Nucl Med* 1990;31:1595–1600.
5. Anderson AR, Friberg HH, Schmidt JF, Hasselbalch SG. Quantitative measurements of cerebral blood flow using SPECT and $^{99m}$Tc-d,l-HM-PAO compared to xenon-133. *J Cereb Blood Flow Metab* 1988;8:S69–S81.
6. Yonekura Y, Nishizawa S, Mukai T, et al. SPECT with $^{99m}$Tc-d,hexamethyl-propylene amine oxime (HM-PAO) compared with regional cerebral blood flow measured by PET: effects of linearization. *J Cereb Blood Flow Metab* 1988;8:S82–S89.
7. Neirinckx R, Canning L, Piper I, et al. Technetium-99m d,l-HM-PAO: a new radiopharmaceutical for SPECT imaging of regional cerebral blood perfusion. *J Nucl Med* 1987;28:191–202.
8. Leveille J, Demonceau G, De Roo M, et al. Characterization of $^{99m}$Tc-L,L-ECD for brain perfusion imaging. Part 2. Biodistribution and brain imaging in humans. *J Nucl Med* 1989;30:1902–1910.
9. Vallabhajosula S, Zimmerman RE, Picard M, et al. Technetium-99m-ECD: a new brain imaging agent: in vivo kinetics and biodistribution studies in normal human subjects. *J Nucl Med* 1989;30:559–604.
10. Garrett K, Villanueva J, Kuperus J, Giombetti R, Mena I. A comparison of regional cerebral blood flow with Xe-133 to SPECT Tc-99m-ECD [Abstract]. *J Nucl Med* 1988;29:913.
11. Moretti JL, Defer G, Cinotti L, Cesaro P, Vigneron N, Pethe C. Comparative tomoscintigraphic study of strokes using ECD Tc-99m, HMPAO Tc-99m and IMP I-123, preliminary results [Abstract]. *Eur J Nucl Med* 1988;14(5/6):311.
12. Devous MD, Leroy RF, Payne JK, Lorimer MK, Bonte FJ. Comparison of Tc-99m-ECD to Xe-133 in the SPECT determination of regional cerebral blood flow in patients with mild perfusion abnormalities [Abstract]. *J Nucl Med* 1990;31:817.
13. Holman BL, Hellman RS, Goldsmith SJ, et al. Biodistribution, dosimetry, and clinical evaluation of Tc-99m ethyl cysteinate dimer (ECD) in normal subjects and in patients with chronic cerebral infarction. *J Nucl Med* 1989;30:599–604.
14. Costa DC, Ell PJ, Cullum ID, et al. The in vivo distribution of $^{99m}$Tc-HM-PAO in normal man. *Nucl Med Commun* 1986;7:647–658.
15. Bruno A, Dosio F, Benti R, et al. Tc-99m ECD: evaluation of a new brain perfusion tracer in humans. *Eur J Nucl Med* 1990;16:S187.
16. Nadler SB, Hidalgo JV, Bloch T. Predication of blood volume in normal human adults. *Surgery* 1962;51:224–232.
17. Castagnoli A, Borsato N, Bruno A, et al. SPECT brain imaging in chronic stroke and dementia: a comparison of Tc-99m-ECD to Tc-99m-HMPAO. In: Hartmann A, Hoyer S, Kuschinski W, eds. *Cerebral ischemia and dementia*. Stuttgart: Springer-Verlag; 1991:327–333.
18. Nakano S, Kazuo K, Jinnouchi S, Hoshi H, Watanabe K. Comparative study of regional cerebral blood flow images by SPECT using xenon-133, iodine-123-IMP, and technetium-99m-HM-PAO. *J Nucl Med* 1989;30:157–164.
19. Neirinckx RD, Burke JF, Harrison RC, Forster AM, Anderson AR, Lassen NA. The retention mechanism of technetium-99m-HM-PAO: intercellular reaction with glutathione. *J Cereb Blood Flow Metab* 1988;8:S4–S12.
20. Walovitch RC, Franceschi M, Picard M. Tc-99m-ECD metabolism of $^{99m}$Tc-L,L-ethyl cysteinate dimer in healthy volunteers. *Neuropharmacology* 1991;30:283–292.
21. Moretti JL, Defer G, Cinotti L, et al. "Luxury perfusion" with $^{99m}$Tc-HMPAO and $^{123}$I-IMP SPECT imaging during the subacute phase of stroke. *Eur J Nucl Med* 1990;16:17–22

## ERRATUM

In the February issue of the *Journal*, Figure 1 in "The Scintigraphic Appearance of Alzheimer's Disease: A Prospective Study Using Technetium-99m-HMPAO SPECT" by Holman et al. was incomplete. The correct figure is printed below.

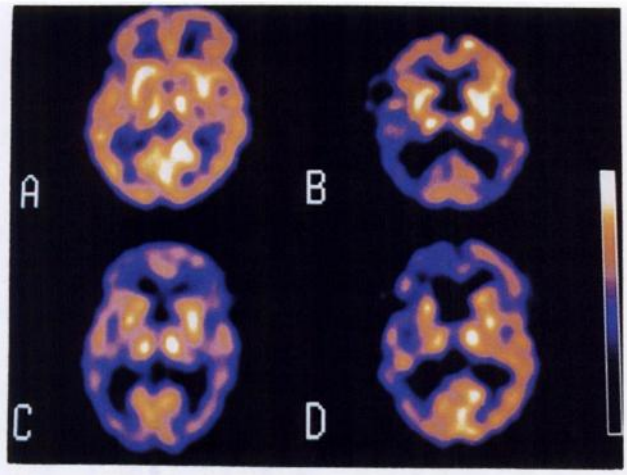


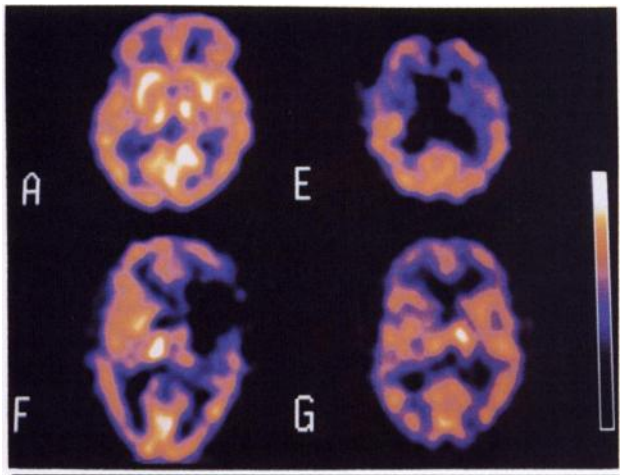


**FIGURE 1.** Examples of $^{99m}$Tc-HMPAO SPECT perfusion patterns. Pattern A: Normal perfusion. Pattern B: Bilateral posterior temporal and parietal defects. Pattern C: Bilateral posterior temporal and parietal defects with additional frontal defects. Pattern D: Left temporal, parietal and frontal cortex defects. Pattern E: Extensive bilateral frontal defects. Pattern F: Large defect involving the right lateral frontal and anterior temporal lobes. Pattern G: Multiple small cortical defects.

(A) Normal.
(B) Bilateral posterior temporal and/or parietal cortex defects.
(C) Bilateral posterior temporal and/or parietal cortex defects with additional defects.
(D) Unilateral posterior temporal and/or parietal. cortex defects with or without additional defects.
(E) Frontal cortex defects only.
(F) Other large (>1 cm) defects.
(G) Multiple small (≤1 cm) cortical defects.